Applied Surface Science 349 (2015) 673–682

Contents lists available at ScienceDirect

Applied Surface Science

journal homepage: www.elsevier.com/locate/apsusc

Highly-conformal p-type copper(I) oxide (Cu_2O) thin films by atomic layer deposition using a fluorine-free amino-alkoxide precursor

Hangil Kim [a], Min Young Lee [a], Soo-Hyun Kim [a,*], So Ik Bae [b], Kyung Yong Ko [c], Hyungjun Kim [c], Kyeong-Woo Kwon [d], Jin-Ha Hwang [d], Do-Joong Lee [e]

[a] School of Materials Science and Engineering, Yeungnam University, 214-1, Dae-dong, Gyeongsan-si 712-749, Republic of Korea
[b] Global Frontier R&D Center for Hybrid Interface Materials, Busan 609-735, Republic of Korea
[c] School of Electrical Engineering, Yonsei University, 50 Yonsei-Ro. Seodaemun-Gu, Seoul 120-749, Republic of Korea
[d] Department of Materials Science & Engineering, Hongik University, Seoul 121-791, Republic of Korea
[e] School of Engineering, Brown University, Providence, RI 02912, United States

ARTICLE INFO

Article history:
Received 29 September 2014
Received in revised form 24 April 2015
Accepted 4 May 2015
Available online 20 May 2015

Keywords:
Cu_2O thin films
Atomic layer deposition
p-Type semiconductor
Conformality

ABSTRACT

A highly-conformal and stoichiometric p-type cuprous copper(I) oxide (Cu_2O) thin films were grown using atomic layer deposition (ALD) by a fluorine-free amino-alkoxide Cu precursor, bis(1-dimethylamino-2-methyl-2-butoxy)copper ($C_{14}H_{32}N_2O_2Cu$), and water vapor (H_2O). Among tested deposition temperatures ranging from 120 to 240 °C, a self-limited film growth was clearly confirmed for both precursor and reactant pulsing times at 140 °C. Between 140 and 160 °C, the process exhibited an almost constant growth rate of ~0.013 nm/cycle and a negligible number of incubation cycles (approximately 6 cycles). The Cu_2O films deposited at the optimal temperature (e.g. 140 °C) showed better properties in view of their crystallinity and roughness compared to the films deposited at higher temperatures. Rutherford backscattering spectrometry showed that the film deposited at 140 °C was almost stoichiometric (a ratio of Cu and O ~2: 1.1) with negligible C and N impurities. X-ray photoelectron spectroscopy further revealed that Cu and O in the film mostly formed Cu_2O bonding rather than CuO bonding. Plan-view transmission electron microscopy analysis showed formation of densely packed crystal grains with a cubic crystal structure of cuprous Cu_2O. The step coverage of ALD-Cu_2O film was remarkable, approximately 100%, over 1.14-μm-high Si nanowires with an aspect ratio (AR) of 7.6:1 and onto nano-trenches (top opening width: 25 nm) with an AR of 4.5:1. Spectroscopic ellipsometry was employed to determine optical constants, giving optical direct band gap of 2.52 eV. Finally, Hall measurement confirmed that the ALD-Cu_2O film had p-type carriers with a high Hall mobility of 8.05 $cm^2/V\,s$.

1. Introduction

Copper oxides, with particular regards to the most stable compounds of cuprous oxide (Cu_2O) and cupric oxide (CuO), are very attractive materials due to many interesting and unique properties of p-type semiconducting nature, tunable optical bandgap, non-toxicity, earth-abundant, and low cost. Specifically, Cu_2O and CuO are known to have band gaps of 2.1~2.6 eV and 1.2~2.1 eV [1], carrier concentrations of ~10^{16} cm^{-3} and ~10^{17} cm^{-3}, and hole mobilities of ~100 $cm^2/V\,s$ [2] and ~6.6 $cm^2/V\,s$ [3] at room temperature (293 K), respectively. As imaginable from the properties listed above, cuprous Cu_2O has a higher mobility and is mostly transparent to the visible rays (around 400–760 nm) while cupric CuO is not transparent because of its small optical bandgap. Owing to these better properties, Cu_2O has been mostly in concern for many applications, including, but not limited to, gas sensors [3,4], resistive random access memories [5,6], photodiode [7,8], anode materials in batteries [9–11], p-type channel layer in thin film transistors (TFTs) [2,12], solar cells [21] and catalysts [13]. Even it is clear that obtaining stoichiometric, cuprous Cu_2O is an important task, a very careful and rigorous selection on process conditions is necessary since Cu_2O can be formed in conditions with a very narrow O_2 partial pressure compared to those of Cu and CuO, as indicated in the equilibrium phase diagram [15]. In fact, during sputtering and chemical vapor deposition, it was reported that a single phase Cu_2O thin film was obtained only in limited conditions of oxygen partial pressure and deposition temperature, while both Cu_2O and CuO were typically formed when deposition temperature or oxygen

* Corresponding author. Tel.: +82 53 810 2472; fax: +82 53 810 4628.
E-mail address: soohyun@ynu.ac.kr (S.-H. Kim).

http://dx.doi.org/10.1016/j.apsusc.2015.05.062
0169-4332/

partial pressure was high [3,16]. In order to deposit Cu_2O thin films, various techniques such as sputtering [2,15], CVD [16,17], electrodeposition [18], pulsed laser deposition (PLD) [19] and thermal evaporation [20] were introduced for many potential applications. These techniques could successfully prepare highly pure p-type Cu_2O thin films upon precise control of deposition parameters. However, these methods have an inherent limitation to be applied for potential higher performance devices with very complex, small-sized, and high aspect ratio structures. To overcome these obstacles, atomic layer deposition (ALD) can give a viable solution for deposition of Cu_2O thin films onto those emerging applications since ALD can provide an excellent conformality, a digital controllability of a film thickness, and a perfect large-area uniformity owing to its inherent surface-saturated and self-limited reaction mechanisms.

In spite of potential strong needs, very few studies have been reported to develop ALD-Cu_2O processes [22–26]. In these studies, both fluorine-containing and non-fluorinated Cu precursors were used, as summarized in Table 1. Generally, fluorine-containing precursors, (trimethylvinylsilyl) hexafluoroacetylacetonato copper(I) [Cu(I)(hfac)(TMVS)] [22] and hexafluoroacetylacetonate copper(I) acetylacetonate [(hfac)Cu(I)(DMB)] [23], have a high vapor pressure of 1 Torr at 60 °C and 2 Torr at 40 °C, respectively, which is desirable for facile delivery of the precursors. By using these precursors, high growth rates of 0.025 nm/cycle at 225 °C with Cu(I)(hfac)(TMVS) and of 0.086 nm/cycle at 100 °C with (hfac)Cu(I)(DMB) were obtained. In addition, excellent electrical properties, such as 5 cm^2/V s and 37 cm^2/V s of mobility and 10^{16} cm^{-3} and 10^{14} cm^{-3} of carrier concentrations, were obtained using Cu(I)(hfac)(TMVS) and (hfac)Cu(I)(DMB), respectively. In those reports, it should be noted that a phase of ALD-grown copper oxide thin films significantly affected by both a reactant pulsing condition and a deposition temperature. For instance, the pure Cu_2O films were deposited only at optimal oxidation conditions (the number of oxidation steps by oxygen plasma), while either Cu or CuO phases were obtained for poor- and rich-oxidation conditions, respectively [23]. In case of Cu(I)(hfac)(TMVS), the pure Cu_2O phase was obtained only at or below 300 °C, while the CuO phase was started to be detected at 350 °C [22]. Even though the fluorine-containing precursors have been successfully introduced for demonstration of high quality ALD-Cu_2O thin films, one remarkable drawback of those processes is a poor adhesion of the deposited films due to fluorine residues at the interface between substrate [24]. To resolve this problem, non-fluorinated Cu precursors, such as bis(tri- *n*-butylphosphane)copper(I) acetylaceotonate [($^nBu_3P)_2$Cu(acac)] [24] and copper monochloride [CuCl] [25], were tested and resulted in film growth rates of 0.04 nm/cycle at 500 °C and 0.01 nm at 120 °C, respectively. However, both precursors suffered from low volatilities. For instance, CuCl should be heated to very high temperature (>400 °C) and limited its use for a low temperature deposition [26]. In the case of ($^nBu_3P)_2$Cu(acac), its low vapor pressure (0.015 Torr at 98 °C) inevitably required much amount of Ar carrier gas upto ~700 standard cubic centimeter per minute (SCCM). In this study, highly pure and stoichiometric Cu_2O films were deposited by ALD by a new fluorine-free amino-alkoxide Cu precursor, bis(1-dimethylamino-2-methyl-2-butoxy)copper ($C_{14}H_{32}N_2O_2Cu$), and water vapor (H_2O). As addressed, the use of F-free precursor can give a clear advantage on the adhesion, which was a critical drawback of the conventional F-containing precursor, by excluding F residues at the film/substrate interface. In addition, this precursor has a relatively high vapor pressure of 1.2 Torr at 80 °C compared to other fluorine-free Cu precursors. The newly proposed ALD system was tested by depositing Cu_2O films on thermally grown SiO_2 substrates at various substrate temperatures ranging from 120 to 240 °C. We confirmed a self-limited film growth and a linearity upon the number of ALD cycles, as in an ideal ALD process, of the present reaction scheme at the ALD temperature window of 140–160 °C. The deposited films were found to be almost stoichiometric (a ratio of Cu and O ~2:1.1) and to have a cubic crystal structure of Cu_2O. A remarkable conformality was demonstrated by depositing ALD-Cu_2O films over 1.14-μm-long Si nanowires and onto very narrow trenches [an opening width of ~25 nm and an aspect ratio (AR) of ~4.5]. In addition, optical and electrical properties of ALD-Cu_2O films were evaluated using spectroscopic ellipsometry and Hall measurement.

2. Experiments

2.1. Deposition

Cu_2O films were deposited using a travelling-wave type ALD reactor (Lucida-D100, NCD technology) with bis(1-dimethylamino-2-methyl-2-butoxy)copper ($C_{14}H_{32}N_2O_2Cu$, 99.9999%) as a precursor and water vapor as a reactant. The new Cu precursor was provided from DNF solution, Korea, and it has a vapor pressure of 1.2 Torr at 80 °C with dark purple liquid at room temperature. Deposition temperatures ranging between 120 and 240 °C were tested to figure out an ALD temperature window of the present ALD scheme. P-type Si (1 0 0) wafers covered with 100-nm-thick thermally grown SiO_2 were used as substrates. The Cu precursor was vaporized in a bubbler at the temperature of 80 °C and was carried into the process chamber by N_2 gas at a flow rate of 200 sccm. The gas delivery line temperature was maintained at 100 °C to prevent condensation of the Cu precursor during the delivery. A water vapor, carried by 100 sccm of N_2 gas, was also provided into the chamber as a reactant. Right after the precursor and reactant pulsing steps, a purging process was performed with 200 sccm of N_2; as in the sequence of the precursor pulsing, purging, reactant pulsing and then purging in each ALD cycle. From preliminary investigations, basic pulsing conditions were set as follows: precursor pulsing for 5 s, reactant pulsing for 5 s and purging for 10 s. Such conditions were found to be sufficient to guarantee a self-limited growth of the ALD-Cu_2O films.

2.2. Analysis of films properties

Thicknesses of the Cu_2O films were determined from analyses of cross-sectional view transmission electron microscopy (XTEM, Tecnai F20 equipped with a 200 kV accelerating voltage and a field emission gun) and X-ray reflectance (XRR, PANalytical X'-pert MRD with Cu-*K*α radiation at 1.5 kW). Properties of the ALD-Cu_2O films according to their deposition conditions were analyzed by using various tools. For phase and crystallinity identifications, grazing-incidence angle (incident angle, $\theta = 3°$) X-ray diffractometry (GIXD, PANalytical X'-pert MRD with Cu-*K*α radiation at 1.5 kW) analysis was performed. A roughness was investigated by using Atomic Force Microscope (AFM, DI Instruments NanoScopeIIIα). A composition and a density were analyzed using a Rutherford backscattering spectrometry (RBS, NEC 2MV Pelletron Accelerator). Resonance RBS techniques were used to accurately detect low-mass elements, such as N and C, in the Cu_2O films. X-ray photoelectron spectroscopy (XPS) analyses were performed to investigate chemical bonding within the Cu_2O films. For XPS study, Al-*K*α of 1204 eV radiation was used and an anode was operated at 15 kV. Plan-view TEM analysis was used to clearly observe microstructures of the ALD-Cu_2O films. Plan-view TEM sample was prepared using conventional procedures, such as tripod polishing and Ar-ion milling. For Ar-ion milling, Gatan precision ion polishing system was used. A conformality of the ALD-Cu_2O films was evaluated both over 1.14-μm-high Si nanowires (AR: ~7.6) and onto trenches with an AR of ~4.5 (top opening width: ~25 nm) by using

Table 1
Summary of reported ALD-Cu_2O processes with various Cu precursors.

	Precursor	Reactant	Growth rate (nm/cycle)	Growth rate (nm/s)	Vapor pressure (Torr)	Note	Refs.
Fluorine-contained Cu precursor	Cu(I)(hfac)(TMVS) [(trimethylvinylsilyl)hexafluoroacetylacetonato copper(I)]	Oxygen	0.025 at 225 °C	0.016	1 at 60 °C	AALD*	[22]
	(hfac)Cu(I)(DMB) [hexafluoroacetylacetonate copper(I)(3,3-dimethyl-1-butane)]	Oxygen	0.086 at 100 °C	0.003	2 at 40 °C	PEALD*	[23]
Fluorine-free Cu precursor	CuCl [copper monochloride]	Water	0.04 at 500 °C	0.004	–	ALD	[25]
	$(^nBu_3P)_2Cu(acac)$ [bis(tri-*n*-butylphosphane)-copper(I)acetylacetonate]	Oxygen + Water	0.01 at 125 °C	0.0003	0.015 at 98 °C	ALD	[24]

* AALD and PE-ALD denote the atmospheric ALD and plasma-enhanced ALD, respectively.

cross-sectional view scanning electron microscope (XSEM, Hitachi S-4800 equipped with a 20 kV accelerating voltage and a field emission electron gun) and XTEM. The optical properties of deposited Cu_2O thin films were analyzed using a spectroscopic ellipsometer (HORIBA, UVISEL, Japan). The optical information pertaining to the amplitude and phase information was measured from 1.5 eV to 5.0 eV at a resolution of 0.05 eV. The obtained amplitude and phase information was analyzed using the commercial software "DeltaPsi 2" (Horiba, Japan). Electrical properties were analyzed using a Hall Measurement (ECOPIA HMS-3000).

3. Results and discussion

3.1. Growth kinetics of ALD-Cu_2O process

Prior to ALD film growths, a thermal decomposition of the new Cu precursor was tested. Only the precursor was pulsed into the chamber at 240 °C for 10 min, without flowing water vapor. In this preliminary test, a film was not grown at all and this indicates that the new Cu precursor is thermally stable up to 240 °C, excluding a possibility of gas phase reaction. Meanwhile, a film was deposited when water vapor was pulsed after precursor pulsing (both for 5 s), indicating that water vapor is essential for growing ALD-Cu_2O films in this study.

Once the thermal stability and reactivity of the Cu precursor was confirmed, a self-limited growth behavior, a key characteristic of an ALD process, was evaluated at a substrate temperature of 140 °C. Fig. 1(a) shows growth rates of the Cu_2O films on thermally grown SiO_2 surfaces as a function of precursor pulsing times. The precursor pulsing times were varied from 3 to 10 s while a reactant pulsing time was fixed to 5 s. The growth rates were determined by dividing the measured film thicknesses by the number of ALD reaction cycles. With increasing the precursor pulsing time from 3 s to 5 s, a growth rate slightly increased to 1.3 times. However, as further increasing the precursor pulsing time, a change of the growth rates became negligible. These results indicate that the ALD growth is self-limiting to the Cu precursor pulsing of 5 s or longer. As similarly, water vapor pulsing times were varied from 1 to 7 s, while the Cu precursor pulsing time was maintained to 5 s, as shown in Fig. 1(b). When the water vapor pulsing time was same as or longer than 5 s, the growth rates showed little change. The same experiment was also done at the substrate temperature of 160 °C [Fig. 1(c)]. The results showed that with increasing the precursor pulsing time longer than 5 s, the growth rates was little changed, which is the same results at the substrate temperature of 140 °C. These results indicate that no thermal self-decomposition of the precursor took place at this temperature and that the deposition was accomplished by a self-limited surface reaction between adsorbed precursors and reactants. Based on the

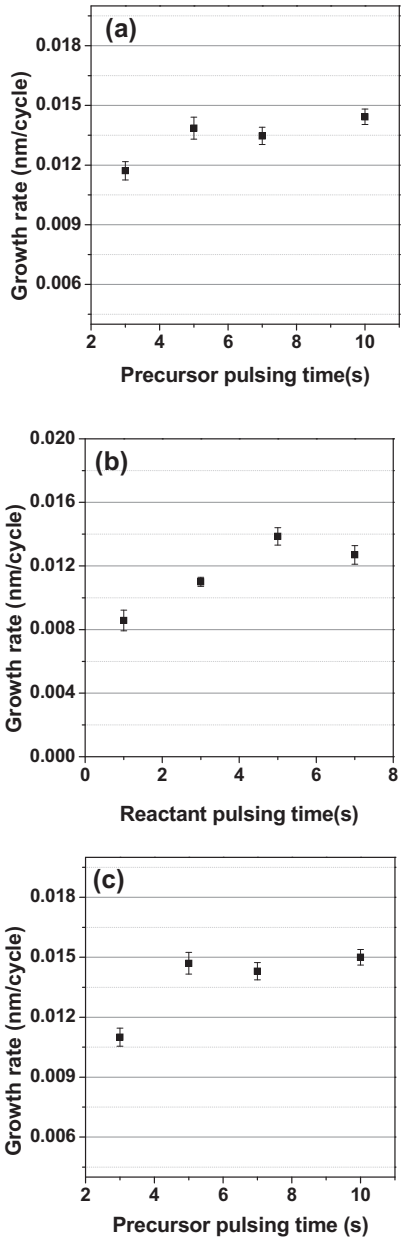

Fig. 1. Growth rates of the ALD-Cu_2O films as a function of (a) precursor and (b) reactant pulsing times at a deposition temperature of 140 °C, and (c) precursor pulsing times at a deposition temperature of 160 °C. Thicknesses were measured by XTEM and the growth rates were defined by dividing the measured film thicknesses by the number of ALD cycles.

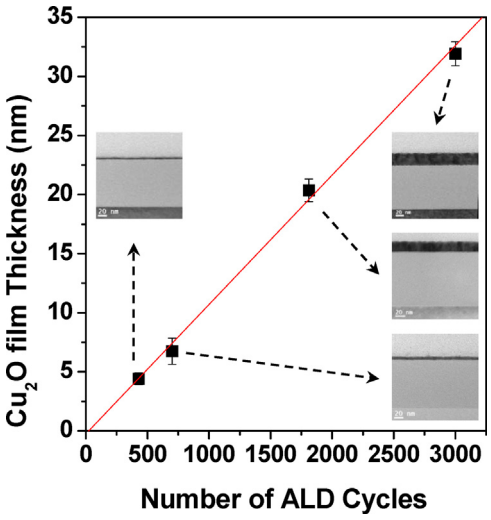

Fig. 2. Thicknesses of the ALD-Cu_2O films as a function of the number of ALD reaction cycles. The films were deposited at 140 °C with the basic pulsing conditions on thermally grown SiO_2 surfaces as substrates. Inset figures show the corresponding XTEM images that were used to measure the film thickness.

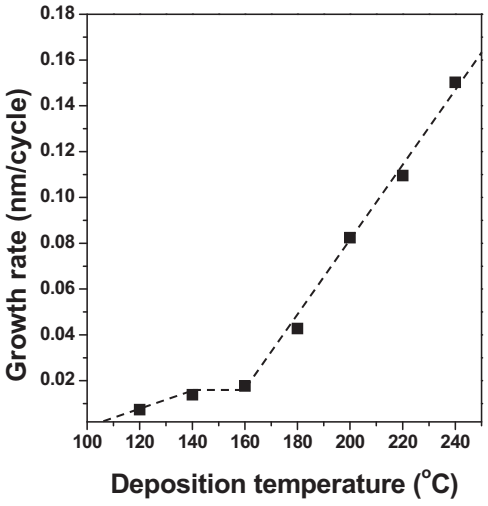

Fig. 3. Growth rates of the ALD-Cu_2O films as a function of a deposition temperature. The basic pulsing conditions that guaranteed the self-limited film growth were used (precursor pulsing of 5 s, reactant pulsing of 5 s, and precursor and reactant purging of 10 s).

results in Fig. 1(a and b), a basic gas pulsing condition, which guarantees the self-limiting and surface-saturated ALD-Cu_2O growth, was set as follows; precursor pulsing for 5 s, precursor purging for 10 s, reactant pulsing for 5 s, and reactant purging for 10 s. Fig. 2 shows thicknesses of the ALD-Cu_2O films deposited on the thermally-grown SiO_2 surfaces as a function of the number of ALD reaction cycles. The films were grown at the deposition temperature of 140 °C and with the basic pulsing conditions set above. The number of deposition cycles was varied from 500 to 3000 cycles. The thicknesses were determined from corresponding XTEM images, as shown in insets of Fig. 2. The film thickness increased linearly with increasing the number of ALD reaction cycles, as in a typical ALD reaction. From a linear fitting of the data points, a growth rate was determined to be 0.013 nm/cycle, which is comparable to the reported value of using $(^nBu_3P)_2Cu(acac)$ precursor [24], while the Cu precursor in this study still holds an advantage of a much higher vapor pressure. In addition, Fig. 2 clearly showed that a very small number of incubation cycles around 6 (defined as an intercept of the extrapolated line with an abscissa) was needed for the growth of ALD-Cu_2O films. Such short incubation period suggests an active adsorption of the Cu precursor molecules and a fast nucleation of the ALD-Cu_2O in this study.

Fig. 3 shows growth rates of the ALD-Cu_2O films, deposited with the basing pulsing conditions (5s–10s–5s–10s), as a function of a deposition temperature. Herein, the growth rates were determined by dividing the measured film thicknesses by the number of ALD reaction cycles. The film deposition at the substrate temperature of 120 °C was possible but its growth rate was too low as ~0.005 nm/cycle. When the deposition temperature increased to 140 °C, the growth rate increased more than twice as ~0.013 nm/cycle. This growth rate was almost constant in the deposition temperatures range between 140 and 160 °C. Further increase of the deposition temperature above 160 °C resulted in a considerable and gradual increase of the growth rate, even up to 0.15 nm/cycle at 240 °C.

3.2. Growth temperature-dependent properties of ALD-Cu_2O films

Properties of the ALD-Cu_2O films deposited at various temperatures were analyzed by using GIXD and AFM to figure out an optimal deposition temperature. Fig. 4 shows GIXD patterns of the ALD-Cu_2O films deposited at 140, 180, and 240 °C. Herein, thicknesses of all ALD-Cu_2O films were the same as ~30 nm. The GIXD results of the Cu_2O film deposited at 140 °C showed specific five peaks corresponding to the cubic Cu_2O. It is noteworthy that no peaks related to CuO or Cu was observed and thereby the film deposited at this temperature consisted of the pure Cu_2O. With increasing the deposition temperature to 240 °C, the peaks intensity of the cubic Cu_2O was decreased remarkably. In other words, the films deposited at lower temperatures exhibited much higher crystallinity, although the growth rates were much lower as compared to those obtained at high deposition temperatures. Such high crystallinity of the ALD-Cu_2O films deposited at low temperature can be a great advantage since it was reported that the crystallinity of Cu_2O thin films significantly affected their electrical properties. For example, Fortunato et al. [2] showed that the mobility of sputter-deposited Cu_2O thin films was significantly improved from 0.65 $cm^2/V\,s$ to 18.5 $cm^2/V\,s$ by post-annealing at 200 °C owing to the improved crystallinity.

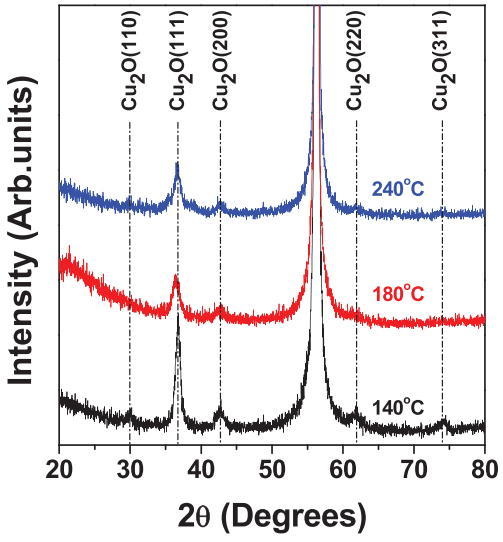

Fig. 4. Grazing incidence angle X-ray diffraction (GIXD) patterns of the ALD-Cu_2O films as a function of the deposition temperature. Thicknesses of the ALD-Cu_2O films were ~30 nm.

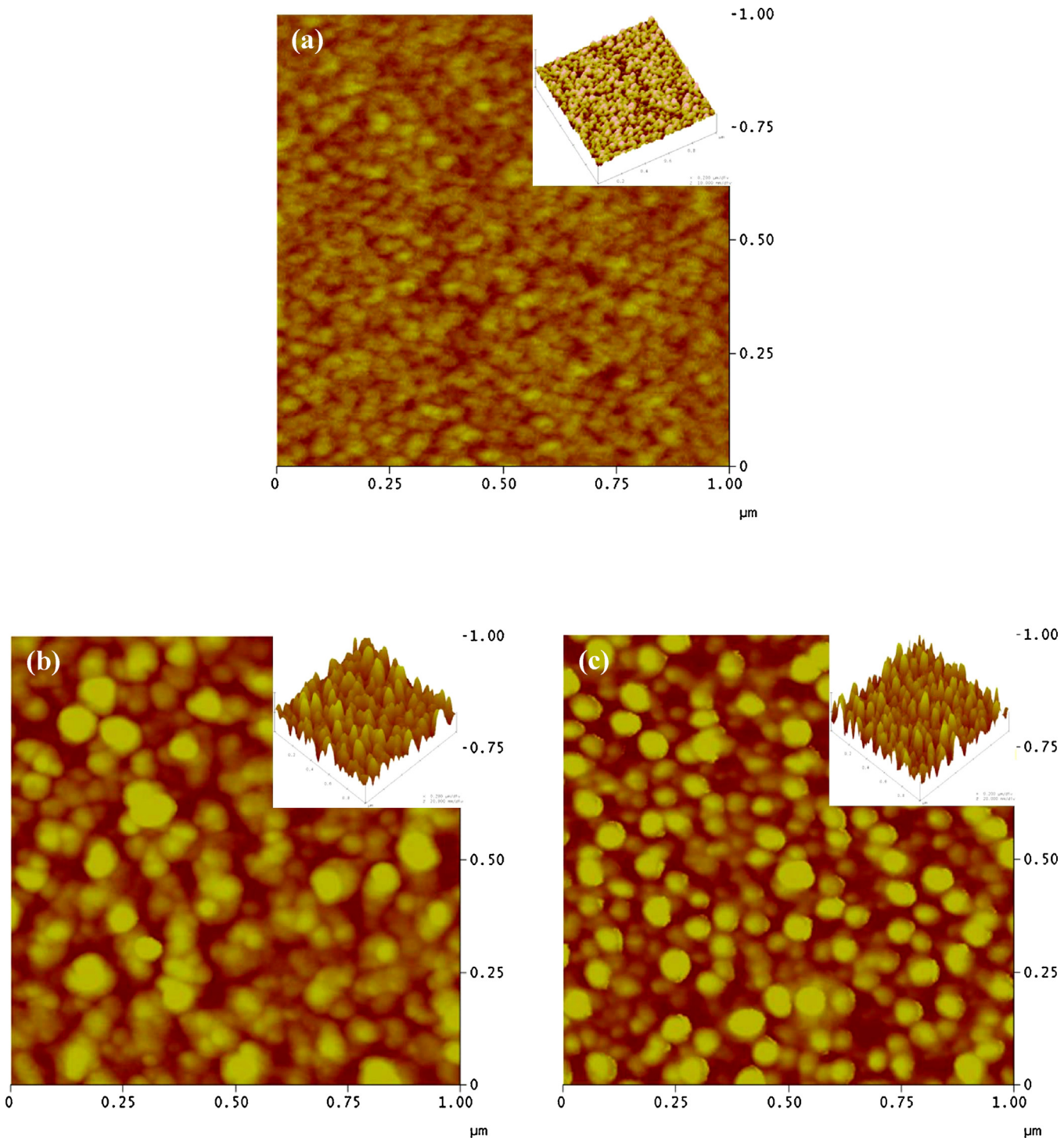

Fig. 5. Atomic force microscope (AFM) results of the ALD-Cu_2O films as a function of the deposition temperature. Thicknesses of the ALD-Cu_2O films were ~30 nm. Inset images show the vertical scaled images.

Roughness of the ALD-Cu_2O films deposited at various temperatures was analyzed by AFM. Fig. 5 shows AFM results of the 30-nm-thick ALD-Cu_2O films deposited at 140, 180, and 240 °C. And inset figures in each Fig. 5(a, b and c) shows the vertical scale AFM results. The Cu_2O deposited at 140 °C has 0.617 nm of roughness. And roughness was increased as increasing deposition temperature from 180 °C to 240 °C. Each temperature has 4.784 nm and 6.084 nm of roughness. The results clearly indicated that AFM roughness of Cu_2O films deposited at high temperatures above the ALD temperature window was much higher than that of the films deposited within ALD temperature window (140 °C), as well as the roughness increased with increasing the deposition temperature from 140 to 240 °C. For instance, a very smooth film with the roughness of 0.617 nm could be prepared at the deposition temperature of 140 °C. Even though the comparison of the roughnesses of ALD-Cu_2O and Cu_2O thin films deposited by other methods, such as sputtering and CVD, is not available due to lack of reported results, the results on the roughness of ALD-Cu and

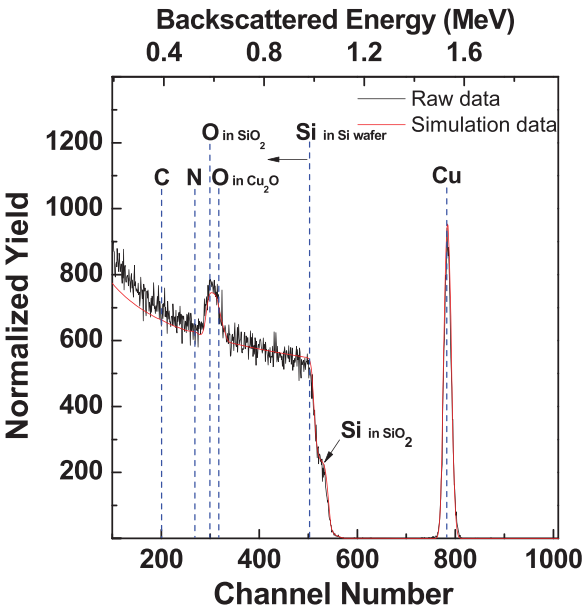

Fig. 6. RBS (incidence energy of He^{2+}: 2 MeV) spectra of the ALD-Cu_2O film deposited on a thermally grown SiO_2 substrate at 140 °C.

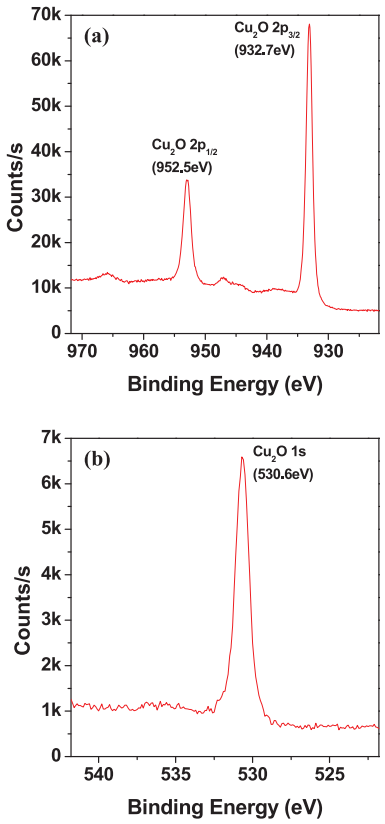

Fig. 7. XPS spectra of the ALD-Cu_2O film deposited at 140 °C with an optimized pulsing conditions (5s–10s–5s–10s); (a) Cu 2p and (b) O 1s.

CVD–Cu [27] might suggest that ALD film generally give a lower roughness. Extremely smooth surface of the film deposited at low temperature (140 °C) can also be observed in the XTEM images in Fig. 2.

The previous paragraphs showed that the properties of the ALD-Cu_2O films deposited at 140 °C, were superior in views of their crystallinity and roughness. Such an availability of the ALD deposition within the temperature window can hold another merit in terms of conformality. Indeed, it was reported that a conformality of ALD films deposited at temperatures above an ALD temperature window was degraded due to thermally decomposed components of a process [28,29]. In fact, considering potential applications of the ALD-Cu_2O films such as a nanowire photodiode composed of p-type and n-type semiconductors [30] and gas sensing [37], preparation of the ALD-Cu_2O films into very small-sized high AR features with an remarkable conformality is essential. In order to meet those requirements, the ALD-Cu_2O films deposited at optimal deposition temperature (140 °C) were further analyzed and characterized, which will be provided in the following section.

3.3. *Properties of ALD-Cu_2O thin film deposited with optimal conditions*

The ALD-Cu_2O films deposited at the optimal conditions (at 140 °C with the basic pulsing conditions) were analyzed by using various tools. First, Rutherford backscattering spectrometry (RBS) analysis was performed to determine a quantitative composition and density and to check a possible incorporation of impurities into the film during the deposition. Fig. 6 shows the RBS spectra of the film (~30 nm) deposited on the SiO_2 (100 nm in thickness) covered Si wafer (~400 μm in thickness). When incident energy of He^{2+} was 2 MeV, as shown in Fig. 6, a backscattering peak from Cu in the deposited film was clearly shown at channel numbers from ~760 to ~810. A backscattering peak from Si consisted of two components; one from the thermally grown SiO_2 at a channel number of ~324 and another from the Si wafer at ~528. A backscattering peak from oxygen was arisen from two different positions as well; one from the SiO_2 and another from the copper oxide film. Using the RUMP simulation, a ratio of Cu and O (Cu/O) in the ALD film was determined as 2:1.1, indicating the almost stoichiometric Cu_2O film. In order to check incorporation of low mass impurities, such as carbon and nitrogen, during the film deposition, both carbon and nitrogen resonance RBS modes with incident He^{2+} energies of 4.282 and 3.7 MeV, respectively, were used (data now shown here). The resonance RBS detected very small backscattering peaks from C and N in the film. The RUMP simulation showed C and N contents were negligible as 0.05 and 0.16 at.%, respectively. A density of the film could also be determined by using the composition data and areal density obtained from RBS, atomic mass of the elements, and the film thickness determined by XTEM. The results indicated that the ALD-Cu_2O film prepared in this study had a very high density of 5.9 g/cm^3, even comparable to a bulk value (6.0 g/cm^3).

The films deposited with the optimal conditions were further analyzed by XPS to identify chemical bonding configurations. A survey spectra, acquired at the film surface in a range of 0–1204 eV of binding energy (not shown here), showed signals of C (due to a surface carbon contamination) as well as Cu and O elements. Thus, XPS data were obtained after sputtering an approximately 4-nm-thick film to remove the surface contamination and to characterize bonding status of the film itself. The XPS data were calibrated to adventitious C 1s peak detected on the film surface. Fig. 7(a) shows the XPS spectrum of Cu 2p orbital. Two intensive peaks centered at around 933 eV and 952 eV were observed and attributed from Cu–O bonding from the cuprous Cu_2O [Cu $2p_{3/2}$: 932.7 eV and Cu $2p_{1/2}$: 952.5 eV] [31,32]. The peak position of Cu $2p_{3/2}$ in this study is consistent with the reported value of ~932.7 eV in the Cu_2O thin films prepared by other method [31]. Very weak satellite located at higher binding energies around 946 and 965 eV were observed and those features could be also identified to Cu–O bonding from the cuprous Cu_2O phase of Cu $2p_{3/2}$ and Cu $2p_{1/2}$ [32]. In case of O 1s XPS spectrum, only a single peak centered at ~530.6 eV was

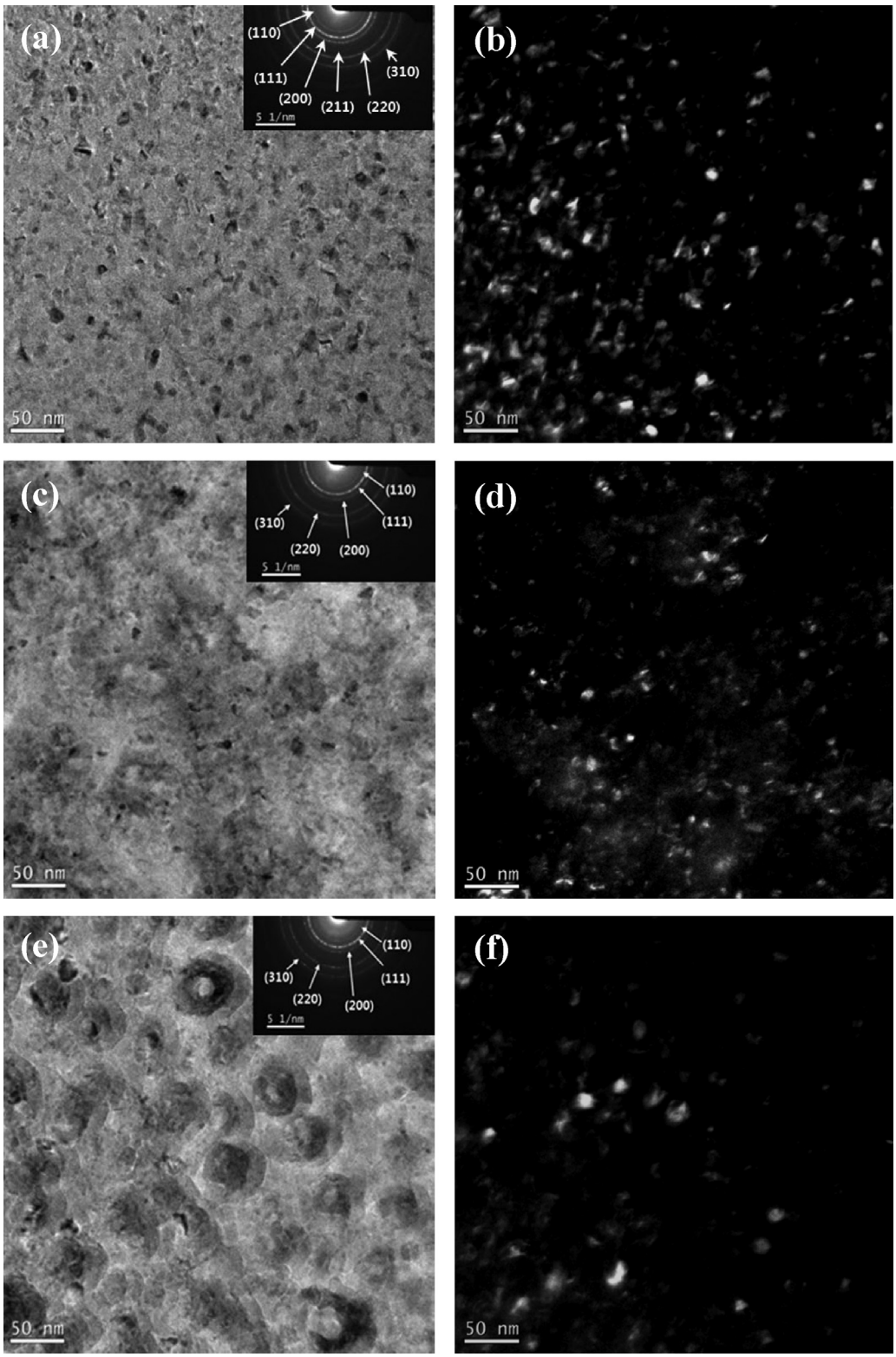

Fig. 8. Plan-view TEM analysis results with deposition temperature; (a) bright-field, (b) dark-field image of the film deposited at 140 °C, (c) bright-field, (d) dark-field image of the film deposited at 180 °C images, (e) bright-field, and (f) dark-field image of the film deposited at 240 °C. The inset figures in (a), (c), and (e) show the selected-area electron diffraction (SAED) patterns at each deposition temperature.

observed, which could be originated from Cu–O bonding in the cuprous Cu_2O. Therefore, the XPS analysis strongly supports that the films deposited with the optimal conditions in this study mostly consisted of the cuprous Cu_2O phase, as corresponding to the XRD results.

Microstructures and phases of the ALD-Cu_2O films were characterized by TEM, as shown in Fig. 8(a–f) [(a and b) deposited at 140 °C, (c and d) at 180 °C, (e) and (f) at 240 °C]. Fig. 8(a, c and e) shows the plan-view TEM bright-field (BF) images of ALD-Cu_2O film with deposition temperature. That clearly showed well-developed

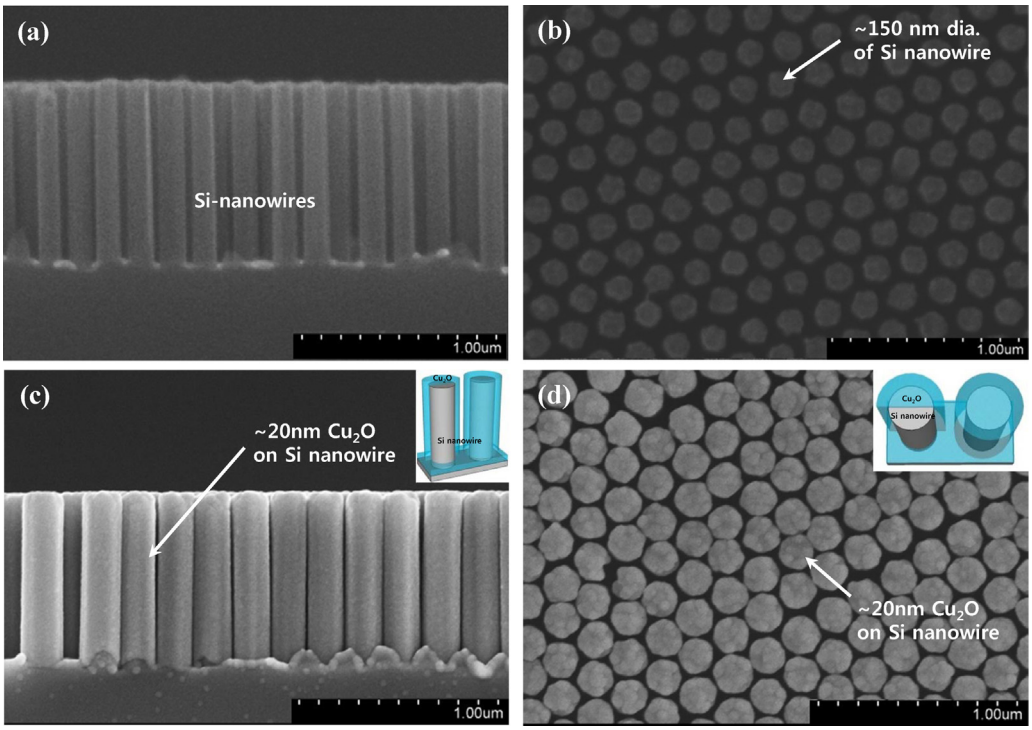

Fig. 9. (a) XSEM and (b) plan-view SEM image of Si nanowire before deposition. (c) XSEM and (d) plan-view SEM image of the ALD-Cu_2O films deposited over 1.14-μm-high Si nanowire (AR ~ 7.6). The inset figures of (c) and (b) showed the schematics of the conformal deposition of ALD-Cu_2O films on high AR Si nanowires.

polycrystalline grains, which were densely packed even though the film was deposited at as low as 140 °C. In the case of ALD-Cu_2O film deposited at 180 °C, it seemed to be difficult to identify individual grains, indicating the degradation of crystallinity as compared to that deposited at 140 °C. In the case of ALD-Cu_2O film deposited at 240 °C, the grains appeared to be somewhat non-homogeneous, which is different from the BF TEM image of the film deposited at 140 °C. The corresponding selected-area electron diffraction (SAED) patterns [inset of Fig. 8 (a, c and e)] suggested that all the films formed the cuprous Cu_2O crystals with the cubic structure (lattice parameter: 4.2696 Å and space group: $Pn\bar{3}m$). From dark-field TEM images [Fig. 8(b, d and f)], which was taken by placing the objective aperture to the first ring of SAED pattern, an average grain size was determined to be around 8.6 nm at 140 °C, 10.27 nm at 180 °C and 24.96 nm at 240 °C. As addressed previously, obtaining a single phase cuprous Cu_2O film was challengeable since a narrow thermodynamic window of Cu_2O typically results in coexistence of Cu_2O with the cupric CuO, even though the cuprous Cu_2O has a clear advantage compared to the cupric CuO in views of its mobility and optical bandgap. It was reported that the CuO phase was formed when the deposition (sputtering) was performed at as high as 350 °C while the Cu_2O phase was formed at 150 °C [22]. Similar phenomena were also shown during preparation of copper oxide using a sol–gel-like dip technique [33]. In the case of ALD copper oxide films, a phase was reported to be greatly dependent on both a reactant pulsing condition [23] and a deposition temperature [22]. Even though those reported processes had limited conditions on obtaining the pure Cu_2O phase, it should be noted that a very pure, stoichiometric and single phase Cu_2O thin film could be readily obtained at low temperature by using the ALD reaction scheme proposed in this study, based on the current investigations of XRD, RBS, XPS, TEM, and SAED analyses.

Conformality of the ALD-Cu_2O process was evaluated by depositing films over very-small sized Si nanowires (AR: ~7.6) and onto nano-trenches (top opening width of 25 nm and AR of ~4.5) since the conformality is a critical factor for their applications into nano-structured devices such as a nanostructured photodiodes [30,34] and a seed layer with reduction process [35]. Fig. 9(c and d) shows the cross-sectional and plan view SEM image of the 20-nm-thick ALD-Cu_2O films deposited over 1.14 μm-high Si nanowires. Fig. 9(a and b) was shown to compare with Si nanowire before deposition. As clearly shown in the image, the Cu_2O films were deposited uniformly and conformally over all Si nanowires. The inset figures of (c) and (d) showed the schematics of the conformal deposition of ALD-Cu_2O films on Si nanowires. This result might suggest a potential improvement of an efficiency of nanowire photodiodes if the present ALD process is used [38]. Fig. 10 showed the XTEM image of the ALD-Cu_2O films deposited onto the nano-trenches. The enlarged one of the XTEM image (the inset figure) confirmed that the thicknesses of the ALD-Cu_2O films at a top, middle, and bottom of the trenches were almost same as ~20 nm, indicating ~100% step coverage. The remarkable step coverage of the ALD-Cu_2O process on those Si nanowire and nano-scale trenches demonstrated in this study obviously indicates that the Cu_2O film can be conformally coated under the ideal, optimized ALD growth conditions, without suffering from the partial decomposition of the precursor. Spectroscopic ellipsometry was employed to estimate optical constants and optical band gap of the ALD-Cu_2O films. From the spectroscopic ellipsometry measurements, the optical constants, i.e. refractive index (n) and extinction coefficient (k), at various incident photon energies (wavelength: λ) were calculated by using excitonic model [14] and plotted in Fig. 11(a). Among the constants, the obtained extinction coefficients (k) were used to extract absorption coefficient (α) of the film by using a following relation,

$$\alpha = \frac{4\pi k}{\lambda}. \quad (1)$$

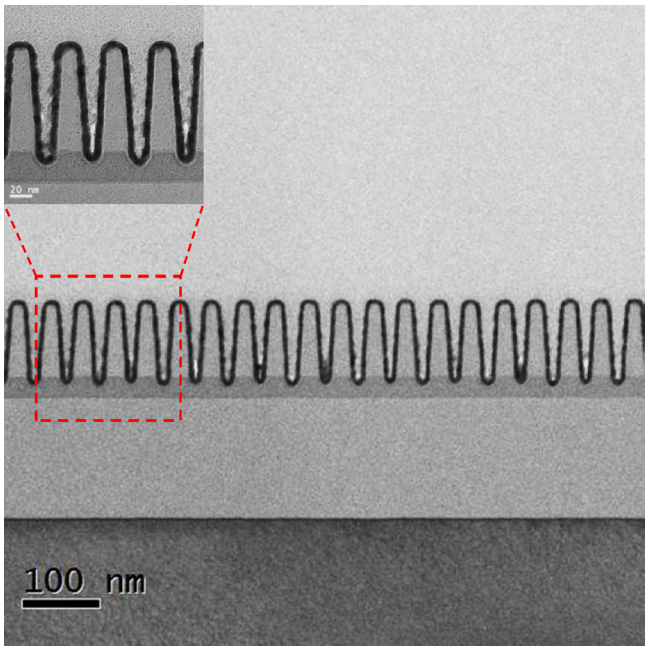

Fig. 10. XTEM image of the ALD-Cu_2O films deposited onto nano-trenches (top opening width: ~25 nm, AR: ~4.5). The inset figure is the enlarged one of the XTEM image.

Those absorption coefficients were further developed to estimate optical bandgap of the ALD-Cu_2O film. As well-known in the Tauc's relationship, frequency-dependence of absorption coefficient is correlated with optical band gap (E_g) of materials [39,40]. The generalized band-gap dependence of the absorption coefficient is given by

$$\alpha h\nu = \left(h\nu - E_g\right)^m. \quad (2)$$

The exponent m is determined depending on a type of band in corresponding semiconductors, i.e. $m=2$ for indirect band gap semiconductors and $m=1/2$ for direct band gap semiconductors. Because Cu_2O is known as a direct band gap material, $m=1/2$ was selected. The plot of $(\alpha h\nu)^2$ versus $h\nu$ gives optical band gap by extrapolating the plot in a linear region to the x-axis, as shown in Fig. 11(b). From the Tauc plot, the optical band gap of ALD-Cu_2O film was estimated to be ~2.52 eV. This value is in reasonable agreement with the theoretical value of 2.4 eV [14] and is also similar compared to those of films deposited by other methods [2,22,36].

Hall measurement was performed to evaluate electrical properties of the ALD-Cu_2O films. The thickness of ALD-Cu_2O film was 100 nm for Hall measurement, and glass was used as insulating substrate to prevent any contribution from the substrate. The Hall measurement confirmed that the films have p-type carriers with a concentration of 5.88×10^{14} cm^{-3}. In addition, the Hall mobility was as high as 8.05 cm^2/V s, which is higher than those of Cu_2O films deposited by sputtering [2] and thermal evaporation [36]. Such superior electrical properties can open a potential for the ALD-Cu_2O films to be used as p-type semiconductors of emerging applications, such as nanostructured photovoltaics and optoelectronic devices.

Finally, the adhesion of ALD-Cu_2O film on SiO_2 substrate was evaluated by using a scratch and peel-off test at a total of 9 points of the wafer. A perfect adhesion of 100% adhesion pass rate was obtained, which is determined by the number of peel-off points out of the total 9 points.

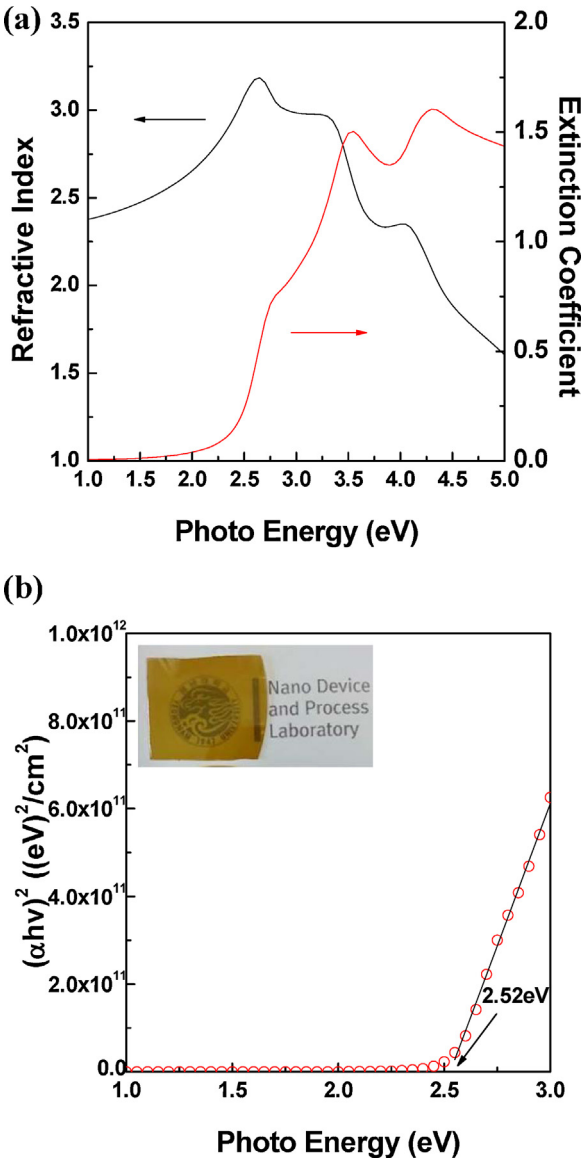

Fig. 11. (a) Refractive index and extinction coefficient obtained from spectroscopic ellipsometry analysis [inset figure shows the actual result of deposited Cu_2O film on glass substrate] and (b) Tauc's plot [$(\alpha h\nu)^2$ *vs.* incident photon energy] for calculating optical band gap of the ALD-Cu_2O film (thickness of the Cu_2O film: 23 nm) The inset figure showed the ALD-Cu_2O film deposited on glass substrate.

4. Summary and conclusions

In this study, the highly conformal and stoichiometric p-type semiconducting Cu_2O thin films were grown by ALD with the sequential supply of the newly synthesized fluorine-free amino-alkoxide Cu precursor, bis(1-dimethylamino-2-methyl-2-butoxy)copper ($C_{14}H_{32}N_2O_2Cu$), and water vapor (H_2O). Among the tested deposition temperatures between 120 and 240 °C, a self-limited film growth behavior was confirmed for both the precursor and reactant pulsing at 140 °C. In addition, between 140 and 160 °C, the growth rate was constant as ~0.013 nm/cycle with the negligible number of incubation cycles. The properties of the ALD-Cu_2O thin films deposited at the optimal temperature (140 °C) were considerably superior to the films deposited at temperatures above the ALD window in views of their crystallinity and roughness. The results based on the XRD, RBS, XPS, TEM, and electron diffraction analysis consistently showed that the very pure (negligible C and N), stoichiometric (the ratio of Cu and O ~ 2:1.1) and single phase

Cu_2O thin film could be easily obtained at a low temperature by the ALD scheme proposed in this study. It should be emphasized that the conformality of the ALD-Cu_2O films was remarkable, approximately 100%, over the very small-sized Si nanowires with AR of 7.6 and trenches with 25 nm-width and AR of 4.5:1. The spectroscopic ellipsometry analysis extracted the optical band gap of the ALD-Cu_2O film as 2.52 eV. Finally, the Hall measurement confirmed that the ALD-Cu_2O films had p-type carriers with a high Hall mobility of 8.05 cm^2/V s. In conclusion, the demonstrated excellent properties of the ALD-Cu_2O films suggest that the present process can be a viable technique for constructing Cu_2O-based emerging semiconductor devices including diodes, photovoltaics, and complementary metal-oxide-semiconductor integrated devices.

Acknowledgements

This study was supported by the Converging Research Center Program through the Ministry of Education, Science and Technology (2012K001298) and also partially supported by Korea Research Foundation (NRF-2012H1B8A2025602).

Appendix A. Supplementary data

Supplementary data associated with this article can be found, in the online version, at http://dx.doi.org/10.1016/j.apsusc.2015.05.062

References

[1] A.A. Ogwu, E. Bouquerel, O. Ademosu, S. Moh, E. Crossan, F. Placido, Appl. Phys. 38 (2005) 266–271.
[2] E. Fortunato, V. Figueiredo, P. Barquinha, E. Elamurugu, R. Barros, Appl. Phys. Lett. 96 (2010) 192102.
[3] K.J. Saji, S. Populoh, A.N. Tiwari, Y.E. Romanyuk, Phys. Status Solidi A 210 (2013) 1386–1391.
[4] J. Zhang, J. Liu, Q. Peng, X. Wang, Y. Li, Chem. Mater. 18 (2006) 867–871.
[5] A. Chen, S. Haddad, Y.C. Wu, T.N. Fang, S. Kaza, Appl. Phys. Lett. 92 (2008) 013503.
[6] W. Yang, W. Kim, S. Rhee, Thin Solid Films 517 (2008) 967–971.
[7] H.T. Hsueh, S.J. Chang, W.Y. Weng, C.L. Hsu, T.J. Hsueh, F.Y. Hung, S.L. Wu, B.T. Dai, IEEE Trans. Nanotechnol. 11 (2012) 1.
[8] R.A. Ismail, Tech. Sci. 9 (2009) 1.
[9] J.Y. Xiang, J.P. Tu, X.H. Huang, Y.Z. Yang, J. Solid State Electrochem. 12 (2008) 941–945.
[10] S. Bijani, M. Gabas, L. Martinez, J.R. Ramos-Barrado, J. Morales, L. Sanchez, Thin Solid Films 515 (2007) 5505–5511.
[11] Q. Pan, M. Wang, J. Electrochem. Soc. 155 (2008) A452–A457.
[12] K. Matsuzaki, K. Nomura, H. Yanagi, T. Kamiya, M. Hirano, Phys. Status Solidi A 206 (2009) 9.
[13] P.E. de Jongh, J. Vanmaekelbergh, J.J. Kelly, Chem. Commun. 24 (1999) 1069–1070.
[14] J. Ghijsen, L.H. Tjeng, J. van Elp, H. Eskes, J. Westerink, G.A. Sawatzky, M.T. Czyzyk, Am. Phys. Soc. 38 (1988) 11322–11330.
[15] C. Chu, H. Lu, C. Lo, C. Lai, Y. Wang, Physica B 404 (2009) 4831–4834.
[16] D. Barreca, E. Comini, A. Gasparotto, C. Maccato, C. Sada, G. Sberveglieri, E. Tondello, Sens. Actuators, B: Chem. 141 (2009) 270–275.
[17] D. Barreca, A. Gasparoto, C. Maccato, E. Tondello, O.I. Lebedev, G.V. Tendeloo, Cryst. Growth Des. 9 (2009) 5.
[18] R. Liu, E.W. Bohannan, J.A. Switzer, F. Oba, F. Ernst, Appl. Phys. Lett. 83 (2003) 1994.
[19] K. Matsuzaki, K. Nomura, H. Yanagi, T. Kamiya, M. Hirano, Appl. Phys. Lett. 93 (2008) 202107.
[20] M.F. Al-Kuhaili, Vacuum 82 (2008) 623–629.
[21] A.T. Marin, D. Aunoz-Rojas, D.C. Iza, T. Gershon, K.P. Musselman, J.L. MacManus-Driscoll, Adv. Funct. Mater. 23 (2013) 3413–3419.
[22] D. Munoz-Rojas, M. Jordan, C. Yeoh, A.T. Marin, A. Kursumovic, AIP Adv. 2 (2012) 042179.
[23] J. Kwon, S. Kwon, T. Jung, K. Nam, K. Chung, D. Kim, J. Park, Appl. Surf. Sci. 285P (2013) 373–379.
[24] T. Waechtler, S. Oswald, N. Roth, A. Jakob, H. Lang, R. Ecke, S.E. Schulz, T. Gessner, A. Moskvinova, S. Schulze, M. Hietschold, J. Electrochem. Soc. 156 (2009) H453–H459.
[25] T. Torndahl, A Study on the Uppsala University in the Sweden, 2004 (Doctor's Thesis).
[26] Z. Li, A. Rahtu, R.G. Gordon, J. Electrochem. Soc. 153 (2006) 11.
[27] J. Huo, R. Solanki, J. Mater. Res. 17 (2002) 9.
[28] S. Kim, J. Kim, J.G. Lee, N. Kwak, J. Kim, S. Jung, M. Hong, S.H. Lee, J. Collins, H. Sohn, J. Electrochem. Soc. 154 (2007) 8.
[29] T.E. Hong, S. Choi, S. Yeo, J. Park, S. Kim, T. Cheon, H. Kim, M. Kim, H. Kim, ECS J. Solid State Sci. Technol. 2 (2013) 3.
[30] H. Kang, J. Park, T. Choi, H. Jung, K.H. Lee, S. Im, H. Kim, Appl. Phys. Lett. 100 (2012) 041117.
[31] A. Chen, H. Long, X. Li, Y. Li, G. Yang, P. Lu, Vacuum 83 (2009) 927–930.
[32] P. Jiang, D. Prendergast, F. Borondics, S. Porsgaard, L. Giovanetti, E. Pach, J. Newberg, H. Bluhm, F. Besenbacher, M. Salmeron, J. Chem. Phys. 138 (2013) 024704.
[33] S.C. Ray, Sol. Energy Mater. Sol. Cells 68 (2001) 307–312.
[34] H.T. Hsueh, S.J. Chang, F.Y. Hung, W.T. Weng, C.L. Hsu, T.J. Hsueh, T.Y. Tsai, B.T. Dai, Superlattices Microstruct. 49 (2011) 572–580.
[35] S. Mueller, T. Waechtler, L. Hofmann, A. Tuchscherer, R. Mothes, O. Gordan, D. Lehmann, F. Haidu, M. Ogiewa, L. Gerlich, S. Ding, S.E. Schulz, T. Gerssner, H. Lang, D.R.T. Zahn, X. Qu, Semiconductor Conference Dresden (SCD), IEEE, 2011, pp. 1–4.
[36] A.H. Jayatissa, K. Guo, A.C. Jayasuriya, Appl. Surf. Sci. 255 (2009) 9474–9479.
[37] N. Datta, N.S. Ramgir, S. Kumar, P. Veerender, M. Kaur, S. Kailasaganapathi, A.K. Debnath, D.K. Aswal, S.K. Gupta, Sens. Actuators, B: Chem. 202 (2014) 1270–1280.
[38] K.Y. Ko, H. Kang, J. Kim, W. Lee, H.S. Lee, S. Im, J.Y. Kang, J. Myoung, H. Kim, S. Kim, H. Kim, Mat. Sci. Semicond. Process. 27 (2014) 297–302.
[39] K. Sato, S. Adachi, J. Appl. Phys. 73 (1993) 926–931.
[40] J. Tauc, Amorphous Liq. Semicond. (1974) 159–220.